Coordinated Multipoint Transmission in Dense Cellular Networks With User-Centric Adaptive Clustering

Virgile Garcia, *Member, IEEE*, Yiqing Zhou, *Senior Member, IEEE*, and Jinglin Shi, *Member, IEEE*

***Abstract*—Based on random network (RN) topologies generated from Poisson point processes (PPP), this paper investigates the performance of macrodiversity coordinated multipoint transmission (MD-CoMP) in dense cellular networks. First, the signal-to-interference-plus-noise ratio (SINR) outage probability is analyzed for a typical mobile station (MS) and for the global network. Next, a user-centric adaptive clustering method is described, which is designed to maximize each MS's normalized outage capacity (goodput). Simulation are carried out and show that MD-CoMP could significantly improve both the RN and regular hexagonal network (HN) coverage performance by increasing the tenth percentile of the SINR by 12 dB if each MS uses a CoMP cluster of size four. It is also shown that MD-CoMP is more beneficial for the RN since 78 MSs in the RN would choose CoMP to optimize their normalized goodput, whereas this number is 58 in the HN. Moreover, 58 MSs in the RN have their normalized goodput doubled compared with that with no CoMP, whereas this number is 36 in the HN. The impact of predefined clustering schemes is also evaluated, to show the importance of using a fully adaptive clustering to overcome cluster-edge issues, where the MSs' performance is poor due to the limited choices of BSs.**

***Index Terms*—Coordinated multipoint transmissions, macrodiversity, random networks, adaptive clustering.**

I. Introduction

DRIVEN by new services, applications and devices, an exponential growth of traffic demand occurs in mobile cellular networks. Despite all improvements that can be performed in different layers of the wireless communications, one dominant factor of gain for the wireless network capacity is the density of access points in the network. A large increase of access points number is presently observed through the deployment of small cells, e.g., personal indoor access (femtocell), street outdoor coverage (picocell), remote radio head (RRH), and so on. This type of deployment breaks the classical paradigm of controlled cellular planning, with pseudo-regular placement of access points and known propagation or coverage. To model this new paradigm, random network (RN) topology has been introduced recently [1]–[4], where mobile stations (MSs) and base stations (BSs) are located randomly in the space. In a RN, the location of each BS or MS is independent to each other, and is assumed to follow a Poisson point process (PPP) distribution. Note that the current real BS deployment could not be accurately modeled by PPP, which is employed mainly for its mathematical tractability. By modeling the dense cellular network as a RN, stochastic geometry theorems can be employed to improve the tractability of large systems, for example by obtaining the global signal-to-interference-plus-noise ratio (SINR) distribution. Thus, important insights could be provided on the performance of practical dense cellular networks. For example, considering general and particular cases of fading, the analytical coverage in a RN is defined in [2]. It is shown that the PPP distribution can be considered as a worst-case scenario of deployment and provides a lower-bound for the performance of current cellular systems [5]. Moreover, heterogeneous networks (HetNets) with multiple tiers of randomly located BSs can also be modeled as a single RN topology [6], and treated with various transmit powers [3]. In dense cellular networks, classical frequency planning to maximize the usage of expensive frequency resources is difficult [3] due to the compact and unplanned topology. Hence, interference becomes an even more serious problem compared to conventional regular cellular networks. Because of the proximity of numerous MSs and BSs in dense cellular networks, a large portion of the cells should be taken as the cell-edge where the MSs experience poor SINR. So interference mitigation is extremely important for the dense cellular system. As an effective scheme to mitigate inter-cell interference (ICI), Coordinated Multiple-Point (CoMP) transmission is concerned in this paper as a key technology for future dense cellular networks.

CoMP is one of the key technologies for the 4th generation (4G) of cellular communication systems. By introducing cooperation among closely located BSs, CoMP could transfer interfering signals into useful signals, thus improve the MSs' SINR, especially at cell edges. There are mainly two categories of CoMP schemes. The first one is the coordinated scheduling/interference avoidance schemes, where the coordinated stations

Manuscript received August 20, 2013; revised January 8, 2014; accepted March 21, 2014. Date of publication April 9, 2014; date of current version August 8, 2014. This work was supported in part by KC Wong Fellowship (the Royal Society), by the Key Program of the National Natural Science Foundation of China under Grant 61331009, by Beijing Natural Science Foundation Major Project under Grant 4110001, and by the 2010 Main Direction Program of Knowledge Innovation of Chinese Academy of Sciences. The associate editor coordinating the review of this paper and approving it for publication was E. Koksal. *(Corresponding author: Y. Zhou.)*

V. Garcia and J. Shi are with the Wireless Technology Research Center, Institute of Computing Technology, Chinese Academy of Sciences, Beijing 100190, China, and also with the Beijing Key Laboratory of Mobile Computing and Pervasive Devices, Chinese Academy of Sciences, Beijing 100190, China (e-mail: virgile.garcia@gmail.com; sjl@ict.ac.cn).

Y. Zhou is with the Wireless Technology Research Center, Institute of Computing Technology, Chinese Academy of Science, Beijing 100190, China, with the Beijing Key Laboratory of Mobile Computing and Pervasive Devices, Chinese Academy of Sciences, Beijing 100190, China, and also with the University of Kent, CT2 7NZ, Canterbury, Kent, U.K. (e-mail: zhouyiqing@ict.ac.cn).

Color versions of one or more of the figures in this paper are available online at http://ieeexplore.ieee.org.

Digital Object Identifier 10.1109/TWC.2014.2316500

perform an interference-aware scheduling, or use MIMO processing to avoid interference to MSs in neighboring cells, e.g., zero forcing (ZF) beamforming [2], [4]. The second one is the joint processing schemes, where the data is transmitted from several BSs simultaneously toward a given MS, using distributed MIMO processing [7]–[12].

Concerning the joint processing in CoMP, although advanced MIMO techniques provide good performance [7], precise and instantaneous channel state information (CSI) is required to be exchanged among the clustered BSs. However, in practice, on one hand, it is difficult for the BSs to obtain accurate downlink CSI, especially in frequency division duplexing (FDD) systems. On the other hand, the backhaul performance is limited. For example, the inter-cell communications between femtocells may have delay issues due to the IP links [13] and instantaneous CSI might not be available. Therefore, considering practical limitations, the CoMP scheme using only statistical CSI would be preferred, such as the open-loop joint processing CoMP scheme, which is employed in this paper to increase the signal strength of cell-edge MSs using macro diversity (MD) gains [8]–[10] and referred to as MD-CoMP.

Although CoMP has been widely investigated in regular hexagonal networks (HN) [9], or linear networks ("Wyner model") [7], [11], there is a limited work on CoMP in RN since dense cellular networks are not the focus of the academy and industry until very recently. Using a multi-cell interference avoidance CoMP with ZF beamforming, the coverage performance of dense cellular networks is studied in [4] using stochastic geometry, where the CoMP uses a hexagonal lattice overlay to cluster BSs together in a static, non-overlapping way. This RN is also investigated in [1] with similar settings but randomly located cluster centers which are generated using an additional PPP. As long as the cluster centers are generated, they will not be changed during communications. Therefore, the clustering schemes in [1], [4] are also static and non-overlapping. However, it has been shown in HN that adaptive and overlapping clustering is more effective due to the increased capability to exploit macro diversity provided by different BSs [8], [9], [14]. In [14], a dynamic non-overlapping clustering is proposed, where the BSs are divided into different disjoint cooperative clusters at each time slot to maximize the uplink system sum-rate for a set of selected MSs. Moreover, user-centric overlapping clusters are shown to be more efficient in [8], for both regular and irregular topologies, but the study is limited to static clustering with three cooperating BSs. In addition, given a regular cellular network with distributed antenna systems, an adaptive clustering scheme is proposed which will select single antenna transmission or cooperative transmission to maximize the normalized capacity [9].

In summary, previous researches in HN have revealed that the user-centric clustering is overlapping and can be adaptive so as to effectively exploit the macro diversity of cooperative BSs. Given the irregular topologies of RN, user-centric adaptive clustering is expected to be even more effective than static clustering. It is necessary to investigate the performance of CoMP in dense cellular networks with user-centric adaptive clustering, which has the potential to enhance the system performance by fully adapting the coordination to each MS's conditions.

In this paper, given the practical MD-CoMP, a performance criterion named normalized goodput (or spectral efficiency, equivalently) is firstly defined for fair comparison. Then the SINR outage probability is analyzed and analytical formulations are obtained for both a single MS and the global network, which can be used to define each MS's outage capacity or the global coverage performance. Next, a user-centric adaptive clustering method is described, which is only based on MSs' local measurements and aims to maximize MSs' normalized goodput. The theoretical network SINR outage probability is verified by simulations. It is shown that MD-CoMP can significantly improve the RN and HN network coverage performance, for example, by increasing the 10th percentile of SINR by 12 dB using 4 cooperative BSs for each user. Then the normalized goodput performance of MD-CoMP with RN and HN topologies is compared in various scenarios. It is shown that MD-CoMP is more beneficial for RN, by compensating the irregularity of BSs locations. For instance, 78 MSs in RN would choose CoMP to optimize their normalized goodput while this number is 58 in HN. Moreover, it is observed that compared to HN, the distribution of optimal cluster sizes of MD-CoMP in RN is relatively uniform, which demonstrates the necessity of adopting user-centric adaptive clustering in RN. The adaptive clustering makes 58 MSs in RN have their normalized goodput doubled compared to that with no-CoMP, while this number is 36 in HN. Finally, it is shown that compared to the predefined PPP clustering, user-centric adaptive clustering will not generate cluster edges in the network where the MSs' performance is poor due to the limited choices of clustering BSs. So it outperforms any fixed or predefined clustering in both RN and HN.

The rest of the paper is organized as follows. We first present the general system model and assumptions in Section II, namely the RN topology, the CoMP joint processing method and the basic metric of interest (goodput) used in this work. In Section III, we derive the SINR outage probability of the MD-CoMP, and provide numerical evaluations of SINR and goodput of the RN. In Section IV, we present the adaptive distributed clustering scheme studied, and Section V regroups the numerical and simulation results to evaluate the system performances in both RN and HN. Finally, conclusions are drawn in Section VI.

Notations: Throughout this paper, we use the following notations. B_Ω represents all the BSs in the system, and U_Ω represents all the MSs in the system. For a given MS $i \in U_\Omega$, we call $b_i \in B_\Omega$ the "primary" station to which it is associated to by default. The primary MSs $U_b \subseteq U_\Omega$ are the MSs that are by default associated to a BS $b \in B_\Omega$. $B_i \subseteq B_\Omega$ is the set of cooperating BSs serving MS i.

II. System Model

A. Topology

A large and dense cellular network is considered in this paper which is modelled by a RN where the BSs' and MSs' locations are placed randomly, following PPP distributions with density parameters of λ_B and λ_M, respectively. Furthermore, the two realizations of the PPPs are assumed to be independent of

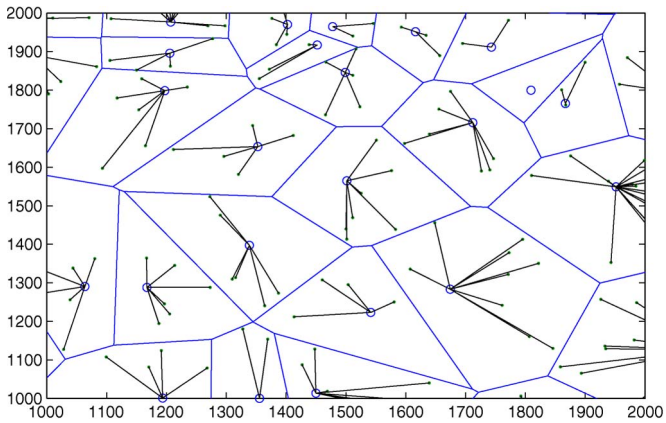

Fig. 1. Illustration of RN topology. Circles are BSs, linked to the MSs (dots). The cell borders are also represented, following the Voronoi tessellation.

each other. Assume that MSs are by default attached to their primary station, noted b_i for MS i, which is the nearest BS since it provides the strongest average signal strength. Using this configuration, the coverage area of each BS is delimited by Voronoi regions [2], as shown in Fig. 1.

B. Signal Model and MD-CoMP

Consider the OFDM-based downlink transmission in a dense cellular network with a frequency reuse factor of one. Single antenna is assumed at both BSs and MSs. The signal received by the MS i on a given resource (e.g., on one subcarrier in one OFDM symbol duration) is given by

$$y_i = \sqrt{P_{b_i}} h_{b_i,i} x_{b_i} + \sum_{b \neq b_i} \sqrt{P_b} h_{b,i} x_b + z_i, \tag{1}$$

where $h_{b,i}$ is the complex channel coefficient between the BS $b \in B_\Omega$ and the MS i, x_b is the complex symbol transmitted with a power P_b by the BS b and z_i is the random additive noise with a variance of σ_z^2. Assume that $h_{b,i}$ is the product of two terms given by $h_{b,i} = \sqrt{l_{b,i}} f_{b,i}$, where $l_{b,i}$ is the path-loss and $f_{b,i}$ is the random fading variable, following a circularly-symmetric complex normal distribution with $\mathbb{E}(|f_{b,i}|^2) = 1$.

In order to use the geometry properties of the RN, the path-loss is only distance dependant, and the large-scale shadowing is not considered. This is equivalent to consider a long-term average path-loss value, similarly as in [2]. Thus, the SINR of a non-cooperative link between b_i and i is given by

$$\gamma_i(b_i) = \frac{P_{b_i} |h_{b_i,i}|^2}{\sum_{b \in B_{\Omega - b_i}} P_b |h_{b,i}|^2 + \sigma_z^2}, \tag{2}$$

where $B_{\Omega - b_i}$ is the set of interfering BSs.

In a practical network, it is difficult for each transmitter to know the instantaneous CSI between all transmitters and receivers, due to channel variations (small scale fading) and network information sharing latency. Therefore, it is supposed in this work that the BSs can only exchange average CSI of their links ($l_{b,i}$), but not the instantaneous value ($f_{b,i}$). Performing a CoMP joint processing without the perfect knowledge of CSI does not allow distributed precoding transmissions nor multiple-user MIMO communications, but allows to exploit the macro diversity of the system, using open-loop MISO schemes [7], [10], [15], and thus is called MD-CoMP. Using Space-Time Coding (STC) transmissions, such as the Alamouti scheme, MD-CoMP does not actually require any CSI knowledge at the cooperating BSs. The knowledge of average channel gain will then only be used for clustering, as shown in Section IV later.

Given B_i as the set of cooperative BSs in the cluster for the MS i and $B_{\Omega - B_i}$ as the set including all other BSs, when a MD-CoMP is employed, the SINR of the received signal is given by

$$\gamma_i(B_i) = \frac{\sum_{b \in B_i} P_b |h_{b,i}|^2}{\sum_{b \in B_{\Omega - B_i}} P_b |h_{b,i}|^2 + \sigma_z^2}. \tag{3}$$

It can be seen that the average signal strength increases with the number of cooperating BSs due to the macro diversity obtained from multiple cooperating BSs. Moreover, the ICI is reduced when more neighbor BSs are transmitting useful signals via cooperation instead of interfering signals. But it should also be noted that the MD-CoMP is a single-user communication technique. When one MS is served by a cluster of BSs on given resources, it imposes that all serving BSs can *not* allocate these resources to any other MS since orthogonal multiuser transmission is assumed within a cell to avoid intra-cell interference. To address this problem, the normalized goodput is introduced.

C. Normalized Goodput

"Goodput" is defined as the capacity that is successfully decoded by the receiver, averaging over the fading [16, Sec. 4.2.3]. Given a SINR threshold γ^* below which the transmitted data cannot be decoded, the goodput is expressed as

$$G(B_i) = \log_2(1 + \gamma^*) \left(1 - p_i^o(\gamma^*, B_i)\right), \tag{4}$$

where $p_i^o(\gamma^*, B_i) = \mathbb{P}\{\gamma_i(B_i) < \gamma^*\}$ is the SINR outage probability of the MS i, which depends on the MS's cluster and the SINR distribution. As discussed before, although the MD-CoMP performs better as the number of clustered BSs increases, the resource availability is reduced accordingly in these BSs. To take the multiple resources consumption into account, the normalized goodput, i.e., the "per station" goodput is employed as efficiency metric [9], [13], [17], which is defined as

$$C_i(B_i) = \frac{G_i(B_i)}{|B_i|}. \tag{5}$$

This normalized goodput can also be interpreted as the performance of MD-CoMP with simplified resource sharing among $|B_i|$ MSs. For example, if $|B_i| = 2$, it means that there are two MSs in two neighboring cells using MD-CoMP. The original resource is orthogonally and evenly shared by the two MSs and $C_i(B_i)$ is the average normalized goodput of the two MSs. Therefore, $C_i(B_i)$ can introduce a balance between the capacity and the resource availability.

It can be seen from (4) and (5) that the normalized goodput is decided by the number of clustered BSs, SINR threshold γ^*, and the SINR outage probability. According to various quality of services (QoS) requirements of different applications, γ^* can be designed with different criteria. In this paper, a transmission mode with fixed outage criterion (FOC) is considered, which is employed when MSs need real time services such as calls or video streaming, and require a low packet error rate to avoid the delay of retransmission. With FOC, a maximum outage probability p^* is given, and then the corresponding SINR threshold γ^* can be obtained from

$$\gamma^* = \max_{\gamma} \{\gamma | p_i^o(\gamma, B_i) \leq p^*\}. \quad (6)$$

Hence, as long as the relationship between γ and the SINR outage probability $p_i^o(\gamma, B_i)$ is known, the SINR threshold γ^* can be obtained by numerical search using the design criteria. Then the normalized goodput can be calculated using (4) and (5).

III. SINR Outage Probability

A. Individual SINR Outage Probability

As can be seen from (4) and (6), the individual SINR outage probability of a given MS i, $p_i^o(\gamma^*, B_i)$, is the key to evaluate the normalized goodput performance. Given the realization of BS locations, the channels between a MS i and the clustered BSs are assumed to experience a Rayleigh fading, thus $|h_{b,i}|^2$ follows a Chi-square distribution of degree two and mean $l_{b,i}$. The average channel gain $l_{b,i}$ can be known at the BSs (through pilot sensing for example). For any realization of the random topology, the individual SINR outage probability of a MS i using MD-CoMP is given by [18]

$$p_i^o(\gamma^*, B_i) = 1 - \sum_{b \in B_i} \left(e^{-\frac{\gamma^* \sigma_z^2}{P_b l_{b,i}}} \prod_{j \in B_i, j \neq b} \frac{P_b l_{b,i}}{P_b l_{b,i} - P_j l_{j,i}} \times \prod_{k \notin B_i} \frac{P_b l_{b,i}}{P_k l_{k,i} \gamma^* + P_b l_{b,i}} \right). \quad (7)$$

From (8), it can be seen that the outage probability depends on the value $P_b l_{b,i}, \forall b$, which is the average power received by the MS i from a station $b \in B_\Omega$. Therefore, it is valid for any kind of topology (e.g., RN, HN), any transmit power (as long as they are known), and can also include measured shadowing in the pathloss. Moreover, although theoretical calculation requires the measure and knowledge of all BSs in B_Ω, practical evaluations using a limited number of accounted BSs are a good trade-off. For instance, a threshold based on the MS's sensitivity can be used to avoid considering BSs that are negligible. It should also be noted that this outage probability shall be used independently for each MS, given their local topologies.

B. Network SINR Outage Probability

Besides the individual SINR outage probability, it is also desirable to obtain the network SINR outage probability of MD-CoMP in RN, which helps to analyze the coverage of the network given the number of BS in a cluster. Consider a MS located at the center of a RN, constructed by a number of BSs whose locations follow a PPP with a parameter of λ_B. Similarly as in [2], a common constant power transmission P_t is assumed for all BSs in the network. Analysis of a network with different transmit powers (e.g., HetNets) will be the subject of a future work.

Focusing on a typical user, the MS index is removed for simplicity. Denote r_b as the distance between a BS b and the MS. The BSs are enumerated according to their distance to the mobile: r_1 is the distance to the primary BS, i.e., the nearest BS to the MS; r_2 the distance to the second nearest BS, and so on, until $r_{|B|}$. Note that $r_{|B|}$ stands for both the farthest cooperating BS and also for the lower bound on the distance to the nearest interfering BS. The average channel gain from a BS b is modeled by $l_b = c r_b^{-\eta}$, with c being the pathloss constant and η the pathloss exponent.

The probability that the communication will be in outage, i.e., probability that the SINR (3) is lower than a threshold γ^* is given by

$$\mathbb{P}\{\gamma(B) < \gamma^*\} = \mathbb{P}\left\{ \sum_{b=1}^{|B|} P_t c r_b^{-\eta} |f_b|^2 < \gamma^* \left(I_{r_{|B|}} + \sigma_z^2 \right) \right\} \quad (8)$$

where $I_{r_{|B|}}$ is the interference received by a MS from the non-cooperating BSs, which should be located at a distance greater than $r_{|B|}$ from the MS.

Theorem 1: For a RN constructed by PPP distributed BSs with a density parameter λ_B, the network SINR outage probability of the MD-CoMP using the $|B|$ nearest BSs is given by

$$\mathbb{P}\{\gamma(B) < \gamma^*\} = 1 - (2\pi\lambda_B)^{|B|} \int_{r_{|B|}=0}^{\infty} \cdots \int_{r_2=0}^{r_3} \int_{r_1=0}^{r_2} \sum_{b=1}^{|B|} \times \left(\frac{L_{I_{r_{|B|}}}(\mu\gamma^* r_b^\eta)\, e^{-\mu\gamma^* \sigma_z^2 r_b^\eta}}{\prod_{j=[1,|B|], j \neq b} \left(1 - \frac{r_j^{-\eta}}{r_b^{-\eta}}\right)} \right) e^{-\pi\lambda_B r_{|B|}^2} \prod_{b=1}^{|B|} (r_b) \mathrm{d}r_1 \cdots \mathrm{d}r_{|B|} \quad (9)$$

where $\mu = 1/(P_t c)$ and $L_{I_{r_{|B|}}}$ is the Laplace transform of the received interference $I_{r_{|B|}}$. See proof and details in Appendix A.

Even if the number of integrations is finite, it may not be trivial to evaluate (9) in the general case. For the ease of numerical evaluations, a particular case with $\eta = 4$ can be considered, where the Laplace transform can be simplified, as shown in (18). Moreover, note that the integration is indefinite in the case where the distances between the MS and two of the cooperating BSs are strictly equal. Since this singularity almost surely does not happen in real environments, numerical or simulation evaluations avoiding these exceptions can be performed without loss of generality.

Given the number of cooperating stations $|B|$, it can be seen from (9) that the outage probability is closely related to $r_{|B|}$, the distance between the MS and the $|B|^{th}$ nearest BS (or the

farthest BS in the cooperative set). First, one can rely on the distribution of $r_{|B|}$ [see (16)] since the distance between the MS and other BSs—interfering and cooperative ones—can be parameterized based on $r_{|B|}$. For instance, in a RN, the remaining B-1 cooperating BSs can be seen as uniformly distributed inside the disk centered at the MS with a radius of $r_{|B|}$, while the interfering BSs are uniformly located outside this disk. Secondly, $r_{|B|}$ sets the limit between cooperative signals and interference signals. In a dense cellular network scenario, the interference overcomes the noise and the network is interference-limited. Thus, avoiding nearby interferences brings a significant gain.

IV. User-Centric Adaptive Clustering

In a wireless cellular network with CoMP, a global coordination is practically impossible. Each MS could be cooperatively served by only a limited number of BSs. Thus, clustering is important to CoMP, deciding which BS(s) serve(s) which MSs. Compared to HN where a clustering with two or three BSs is expected to provide good performances, fixed and predefined clustering methods are obviously not optimal for RN with irregular topologies.

A. Distributed Clustering Criterion

In this paper, a user-centric adaptive clustering is considered, where each MS is able to define its own cluster, based on local measurements only and independently to other MSs' choices. The objective of the clustering scheme is therefore to maximize the normalized goodput, given by

$$B_i^* = \arg\max_{B_i} \frac{\log_2(1+\gamma^*)\,(1-p_i^o(\gamma^*, B_i))}{|B_i|}. \qquad (10)$$

As stated before, MD-CoMP is a single-user MIMO technique, where a resource used to serve a MS cannot be used in any of the cooperating stations for another MS. Thus the cooperation among several BSs limits the reuse of certain resources in the network for other MSs. Choosing the normalized goodput as a criterion could balance the capacity and the resource availability and maximize the equivalent spectral efficiency of each MS. Since the capacity is improved in a logarithmic scale with the SINR, while the efficiency grows inversely proportional to the number of cooperating stations, it is expected that this will naturally limits the clusters' size. Although the formulation of (10) is a generic approach that can be applied to any SU-MIMO kind of CoMP, this paper is focused on the MD-CoMP coordination, and thus (8) is used as the individual outage probability $p_i^o(\gamma^*, B_i)$.

Using MD-CoMP, the goodput depends on the average power received from neighboring BSs. Let a MS sort the neighboring BSs by their received power level and evaluate the performance of various clusters. Since the pathloss model is only distant dependent, the nearest BSs have the strongest signal power level. Thus, the cluster regrouping the $|B|$ nearest BSs is the best cluster of size $|B|$. Therefore, if $B_{\max}$ denotes the maximum cluster size, there are only $B_{\max}$ clusters to compare when solving (10).

Aiming to maximize the normalized goodput of each MS, the optimized cluster size changes with MSs, adapting to each MS's channel conditions. The resultant clusters are overlapping each other, which have been shown to be more efficient than non-overlapping ones [8]. It should also be noted that the adaptation capability comes at the cost of a higher implementation complexity of the system. For instance, CoMP coordination imposes inter-cell cooperation and information exchanges. Using the fully adaptive and overlapped clustering, a BS can belong to two distinct clusters simultaneously. In this case, the inter-BSs communication increases and resource sharing is more complicated.

B. Implementation Aspects

1) Measuring and Sharing Requirements: To apply the user-centric adaptive clustering scheme, the MS should be able to measure the average path-loss of neighboring BSs, which can be done through pilot sensing. Note that similar measurement is already performed for handover procedures, for example. The MS is then required to determine the normalized goodput of any combination of cooperation with the BSs in its surrounding, following (10), and report its clustering choice to its primary BS. Since the computation of (10) is non-trivial, to reduce the complexity at the MS, it can send the channel information to the primary BS to perform the computation. Based on the results obtained from (10), the BSs exchange the necessary information with chosen BSs to start the clustering.

It is worth mentioning that for MD-CoMP using STC techniques, no CSI is to be shared between the cooperating BSs, which relaxes the latency constraints on the inter-BS links. Meanwhile, the data to be delivered to the MS can be distributed to clustering BSs by the operator network directly instead of shared between BSs via backhauls. Of course this requires additional signaling and complicates the management of BSs and MSs.

2) Adaptive vs Predefined Clusters: The main idea of user-centric adaptive clustering is to let MSs be served by any BSs in its neighborhood. However, this leads to the formation of dynamic and overlapping clusters. This imposes flexibility in the communications between the BSs. For example, BSs have to keep a list of potential neighboring BSs to cooperate with, which can be obtained through MS measurements reports (similarly to hand-over). From time to time, this list should be updated in dense cellular networks, whose topology changes when some BSs are temporary deployed in hotspots or small BSs at homes are turned on or off. Using the user-centric adaptive scheme, the clustering will also change to adapt to the updated network topology. On the other hand, the predefined clustering generates fixed and non-overlapped clusters and is simple to realize, but it lacks the capability to adapt to the network changes and the performance is inferior to that with the adaptive scheme.

The inter-cell resource sharing is also an issue for CoMP systems. Orthogonal resource sharing, which is necessary for the MD-CoMP, imposes a resource scheduling for several BSs. This creates inter-cell allocation constraints. In fixed non-overlapping clusters, this may not be a very difficult task

TABLE I
SIMULATION PARAMETERS

Parameter	Value
BS density (λ_B)	28BS/km^2
MS density (λ_M)	280BS/km^2
RB bandwidth	200kHz
Thermal noise	-174dBm/Hz
Feeder loss (MS and BS)	5dB, 7dB
Noise for a RB (σ_z^2),incl. feeder	-109dBm
BS total power + antennas gain	44dBm + 16dBi
Transmit power per RB (P_t)	40dBm
Pathloss (l), d in meters	33.05+36.7 $\log_{10}(d)$
Number of MSs	10000
Maximum cluster size (B_{max})	8

since the constraints are bounded inside the cluster. However, using user-centric adaptive clustering, these constraints become unbounded. Fortunately, this problem can be solved through distributed graph coloring algorithms [19]. Since this paper focuses on the outage performance of MD-CoMP in dense cellular networks and clustering schemes, the resource sharing is not considered here and it is assumed that each MS can be allocated to at least one resource by its serving cluster.

V. NUMERICAL EVALUATIONS

Numerical computation and simulations are carried out to evaluate the performance of MD-CoMP in dense cellular networks with user-centric adaptive clustering. The ITU-R urban micro-cell settings are employed [20], and the NLOS channel model is considered. For the RN, BSs, and MSs are uniformly and randomly located on a plane according to two independently generated PPPs, with parameters $\lambda_B = 28$ BSs/km^2 and $\lambda_M = 280$ MSs/km^2, respectively. This setting gives an average of 10 MSs per BS.

In the following, except specified otherwise, the results have been obtained using a very large area, where a total of 10 000 MSs are located, and using parameters summarized in Table I. These large settings have been motivated to avoid any border effect. For the HN with hexagonal topology for comparison, the BSs are located on an hexagonal grid with a 200 m inter-site distance (equivalent to $\lambda_B = 28$ BSs/km^2) and MSs are placed similarly as in the RN topology. Using such parameters, the MSs' simulated area is a 6 km * 6 km square plan. Moreover, the area used to generate the BSs has been set to be 1 km larger than the MSs' area on each side, i.e., a 8 km * 8 km square plan. Using a 1 km extra margin is made so that a MS on the edge of the simulated MS plan will experience interference from at least BSs inside a disk of radius 1 km (i.e., 88 BSs in average) plus the ones inside the simulated MS area. Thus, in a dense deployment and interference limited scenario, interference from BSs farther away can be neglected.

A. Network SINR Outage Probability

First of all, to verify the analytical results obtained from (9), Fig. 2(a) plots the network SINR outage probabilities obtained from analysis and simulations for the RN topology. The settings used for this evaluation are the ones of Table I, except that the pathloss coefficient has been set to 4, for the ease

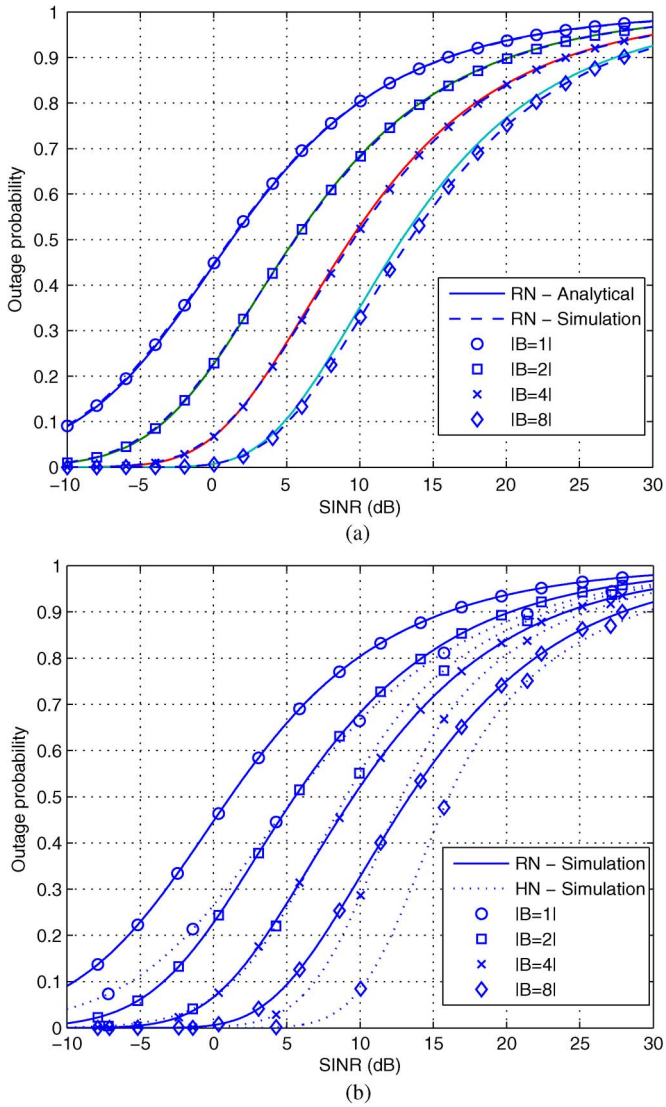

Fig. 2. CDF of the SINR of a typical MS, with a fixed cluster size. (a) Comparison between analytical and simulation results. (b) Comparison between RN and HN topologies.

of numerical evaluation. The numerical integration has been performed averaging 10^5 randomly generated distances sets $r_1 \ldots r_{|B|}$. The simulations results comes from the generation of 1000 random fading states using the simulation topology described previously.

Fixed clusters are employed with different sizes from one to eight. Note that when the cluster size is one, there is no CoMP. It can be seen that the analytical and simulated results almost coincide with each other, demonstrating the effectiveness of (9). A slight mismatch can be observed at larger cluster-size curves, e.g., $|B| = 8$. This is because when $|B|$ increases, the complexity of (9) increases and the accuracy of the integration approximation used in numerical evaluation is limited by the computer memory. Moreover, the SINR performance of the MSs naturally increases with the size of the cooperating set. Additionally, the distributions' tails are reduced as $|B|$ increases, thanks to macro diversity which limits the probability of deep-fading states.

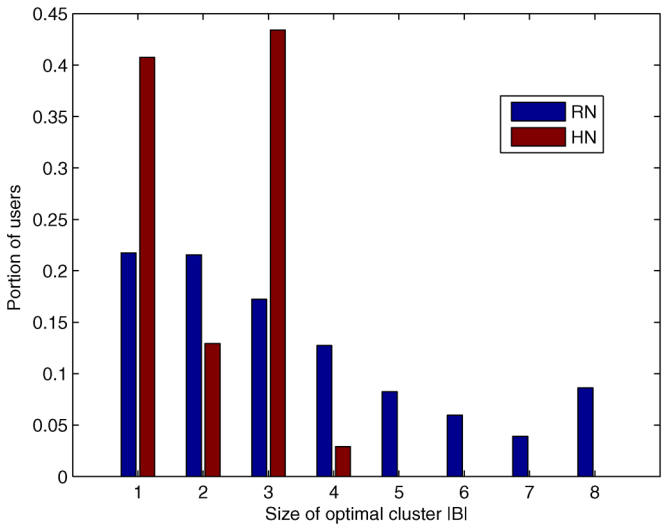

Fig. 3. Distribution of the optimal cluster size in RN and HN.

Fig. 2(b) compares the SINR outage probability in RN and HN topologies. It can be seen that whether CoMP is employed or not, HN outperforms RN. In a dense RN, when there is no CoMP, about 45% of MSs have a SINR smaller than 0 dB, while in a regular one, less than 30% of MSs suffers from a 0 dB or less SINR. The use of MD-CoMP significantly reduces the number of MSs with very low SINR. When using a cluster of size four, the outage probability to reach $\gamma^* = 0$ dB is about 5% in RN, while this number is practically negligible in HN.

Considering the 10th percentile of SINR in the network which stands for the coverage performance, the HN outperforms the RN by 5 to 6 dB for both no-CoMP and CoMP with fixed clustering size. In the RN, the gain provided by MD-CoMP with $|B| = 2$ is 7 dB for the 10th percentile compared to no-CoMP. Using $|B| = 4$ and $|B| = 8$, this gain becomes 12 and 16 dB, respectively. Similar improvements can be observed in HN. It can be seen that the network performance obtained from HN is optimistic and deviates from the real performance when the network becomes more and more unplanned.

B. MD-CoMP With User-Centric Adaptive Clustering

The network SINR outage performance has been shown in Fig. 2, demonstrating the improvement in SINR provided by MD-CoMP with fixed clustering. Please be noted that the CDF of SINR in previous figure represent a global coverage evaluation. This does not correspond to the SINR threshold γ^* when considering the FOC transmission. Since each transmission to MS can use different modulation and data-rate, the threshold γ^* should be defined for each MS. In the following, we use the FOC (6) with $p^* = 10\%$ as a maximal outage probability criterion.

Note that although SINR improves as the cluster size increases, the radio resource occupied also increases. Therefore, considering a more reasonable metric, i.e., normalized goodput, the performance of MD-CoMP with user-centric adaptive clustering is investigated in both RN and HN.

1) Optimal Cluster Size: First of all, Fig. 3 shows the repartition of the size of the optimal cluster chosen by MSs, to maximize their normalized goodput, in both the RN and the HN. In this simulation, the cooperation set size is limited to $|B| = 8$. This limitation has been set as a trade-off between practical considerations and performance improvements, since a very limited number of MSs would increase their normalized efficiency with cooperation higher than eight cells. It can be seen that in dense cellular networks with RN topology, only 22% of MSs use a cluster of size one, i.e., no-CoMP. Therefore, 78% of MSs benefit from MD-CoMP. Moreover, 40% MSs in RN choose clusters with more than three BSs. A sudden spike of intensity is observed for $|B| = 8$ in RN. This is because the maximum cluster size is set to eight, so the MSs that could actually improve their efficiency with more than eight stations often choose eight as the optimal cluster size.

In HN, the ratio of MS using MD-CoMP is 58%, and only 2% of the MSs select a cluster of size four. This is because the regularity of the hexagonal pattern makes the MSs suffer from only one or two dominant interferences with the other neighboring BSs being much farther away. Thus, the cooperation required to reduce the level of interference is only limited to the one or two nearest neighboring BSs. Moreover, it is shown that in HN, the performance maximization is more often associating three BSs than only two, due to the hexagonal geometry of the network. So one can expect that clustering with fixed sizes, e.g., three, could be proper for CoMP in HN. However, it is far from being optimal for CoMP in RN, given that MSs choose different sizes of clusters, to mitigate the interference coming from multiple sources. Therefore, it can be summarized that in RN, the MD-CoMP can bring benefits to a larger number of MSs and, each MS should be allowed to set up its cluster optimally. Thus, the user-centric dynamic clustering is needed.

2) Distribution of Normalized Goodput: Fig. 4 shows the CDF of normalized goodput C of MSs in both RN and HN. The CDF performances with fixed cluster of size 1, 2, 4, and 8 are compared to that with the user-centric adaptive clustering [see (10)]. First of all, it can be seen that the normalized goodput performance is quite different from the SINR outage performance shown in Fig. 2. The SINR outage probability reduces as $|B|$ increases because the received SINR gets better. However, more resources are occupied by MD-CoMP when $|B|$ gets larger. Therefore, the normalized goodput could be degraded by a larger $|B|$, as shown in Fig. 4. Moreover, it is observed that compared to CoMP with fixed cluster-size, the non-cooperative scheme ($|B| = 1$) provides not only a larger number of MSs with a lower normalized goodput (i.e., spectral efficiency), but also a larger number of MSs with a higher normalized goodput. For example, considering RN, there are about 53%, 28%, 20% and 18% of all MSs having a normalized goodput of less than 0.2 bps/Hz with $|B| = 1, 2, 4,$ and 8, respectively, while the numbers become 13%, 12%, 5% and 1% concerning MSs having a normalized goodput higher than 1.5 bps/Hz.

This is because although cooperation introduced by CoMP could improve the received SINR of MSs, it is obtained at the cost of less resource availability. For cell-edge MSs with low normalized goodput, the gain in SINR is significant and compensates the loss in resource availability. Hence, their normalized goodput is improved by CoMP. On the other hand,

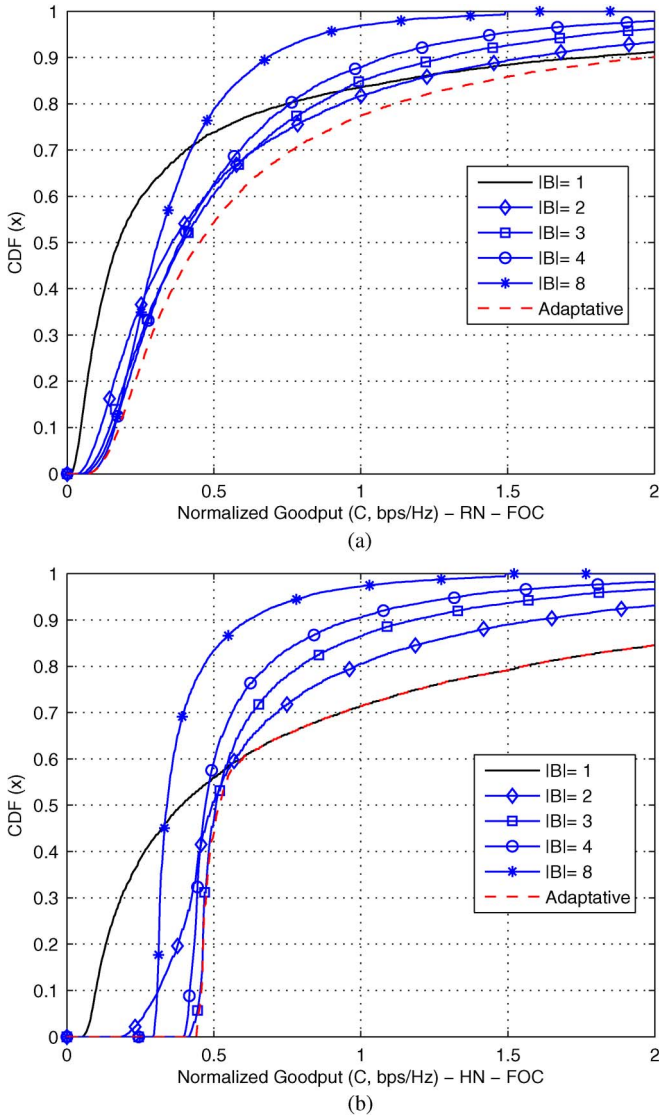

Fig. 4. CDF of normalized goodput received by MSs. (a) RN. (b) HN.

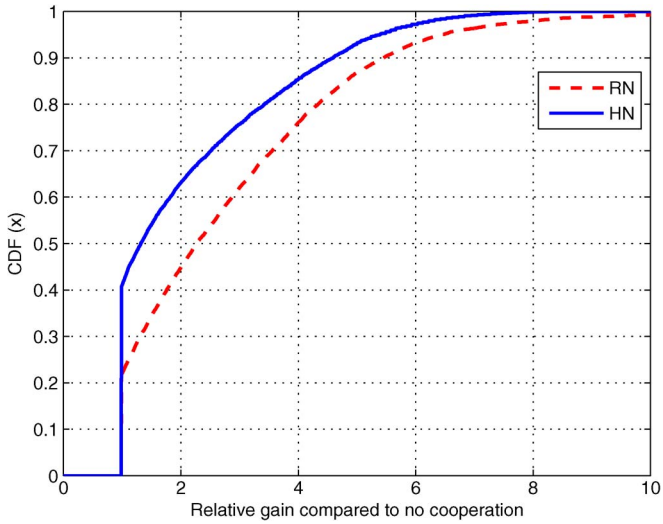

Fig. 5. Distribution of the relative gain in normalized goodput of CoMP compared to No-CoMP.

for cell-center MSs, they experience good channel conditions and the SINR improvement provided by cooperation does not compensate for the $1/B$ factor in the normalized goodput. Therefore, with MD-CoMP, the normalized goodput of cell-center MSs is reduced. So it can be seen that to optimize its performance, each MS should choose different CoMP sizes. This demonstrates the necessity to adopt user-centric dynamic clustering. As shown in Fig. 4, the user-centric adaptive clustering outperforms the clustering with fixed sizes, for both topologies.

It is also interesting to see that in HN, the CDF with user-centric adaptive clustering is close to that of $|B| = 3$ when the normalized goodput is low, then the curve increases rapidly and coincides with that of no-CoMP. It means that in HN, the performance of user-centric adaptive clustering can be closely approximated by a simplified scheme with clustering of constant size and proper user grouping, where all MSs are firstly grouped into cell-edge MSs and cell-center MSs, then cell-edge MSs should employ a CoMP with fixed clustering of size three and cell-center MSs should not use CoMP. Note that to be efficient, this scheme still need to be overlapping. The three-cell CoMP is one of the techniques recommended by the 3GPP to perform coordination, for both the intra-site and inter-site coordination [21]. However, this kind of close approximation does not hold in RN due to the geometry. Therefore, user-centric adaptive clustering is more necessary in RN than in HN.

3) Relative Gain in Normalized Goodput: Fig. 5 shows the distribution of gains in normalized goodput of CoMP compared to the non-cooperative case, i.e., $C(B_i)/C(b_i) = G(B_i)/G(b_i)|B_i|$, for both RN and HN. It can be seen that the relative gains brought by CoMP in RN are more advantageous than that in the HN. For example, 58% of the MSs in RN have a spectral efficiency at least doubled, while this number is only 36% in HN. Considering that the performance of HN is an optimistic estimation for practical networks and that of the RN is a worst-case scenario [5], Fig. 5 provides the possible gain range of normalized goodput provided by MD-CoMP that can occur in any arbitrary topology. It is also worth noticing that the relative gain reached cannot be less than one since the adaptive clustering will choose the best cluster size for each MS. Therefore, if no cooperation is needed, the MS will use the traditional non-cooperative transmission.

From Figs. 4 and 5, it can be concluded that compared to HN, RN can benefit more from cooperative communication and user-centric adaptive clustering. This is because RN is irregular with more areas in the network with high levels of interference. So there is a higher need for cooperation.

4) Impact of BS Density: In this subsection, we study the BS density λ_B, to see impact of the interference limited regime on the system. Note that for this simulation results, the area simulated for the BSs has been set accordingly to its density, to avoid border effect. More specifically, the margin on each side is set to be $10/\sqrt{\lambda_B}$ km, to ensure a large number of BSs for interference coverage.

Fig. 6 shows the evolution of the 5th percentiles and the average of the normalized goodput as a function of the BS density in both RN and HN. Since the normalized goodput of a MS is independent on other MSs, the MS density λ_M is

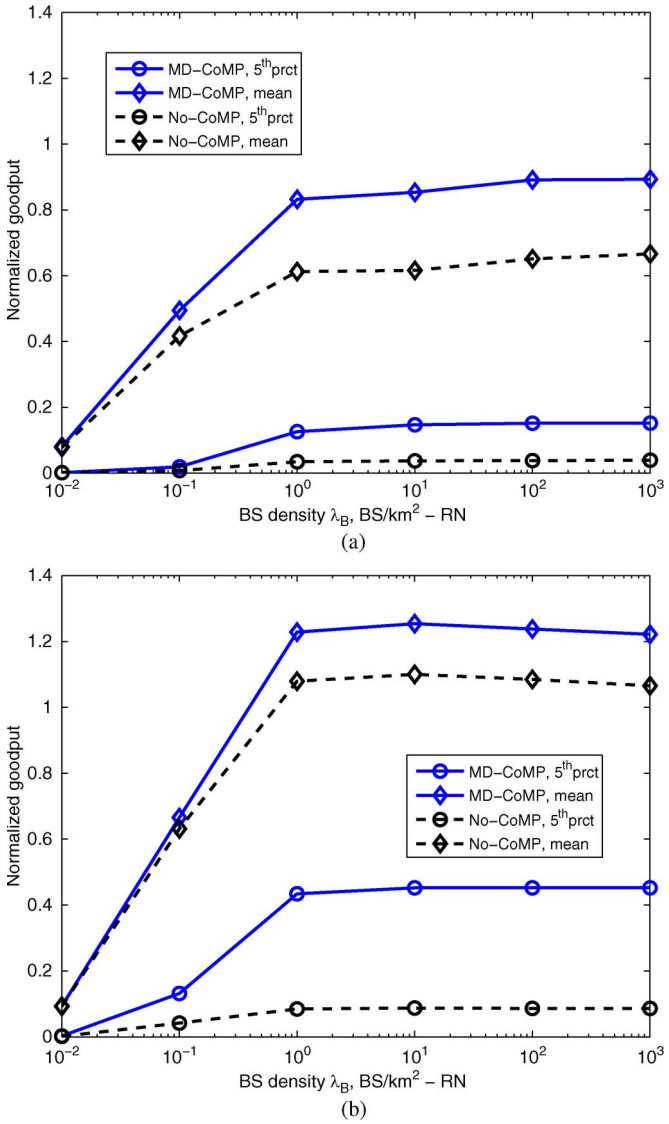

Fig. 6. Normalized goodput as a function of the BS density λ_B. (a) RN. (b) HN.

set to $10\lambda_B$ and the network area is adapted to have 10^4 MSs and a large enough number of BSs to avoid border effects. It is shown that when the BS density increases from 10^{-2} to 1 BS/km^2, the normalized goodput is improved. This is because when the BS density is low, there is little ICI and the system is noise-dominant. When the BS density increases, the useful signal becomes stronger as well as ICI due to the reduction of the distance between BSs and MSs. Although the Signal-to-Interference Ratio (SIR) is actually invariant with the density as long as a common power level is used [2], the impact of noise reduces and the SINR improves, resulting in a better normalized goodput. Moreover, as the BS density is further increased beyond $\lambda_B = 1$ BS/km^2, there is no much change in the normalized goodput and the performance is stable. The reason is that the system becomes interference limited when the BS density is larger than 1 BS/km^2. In this case, noise is negligible compared to interference. So both the SIR and SINR are constant with the increasing density, resulting in the invariant normalized goodput.

The gain brought by MD-CoMP over No-CoMP also increases with the BS density until the saturation, demonstrating that cooperation is more efficient in interference limited systems. In RN, concerning the 5th percentile of the normalized goodput, the gain is 140% when $\lambda_B = 0.1$ (low ICI) and 299% when $\lambda_B = 10$ (interference limited). The gain of the average normalized goodput is 19% with $\lambda_B = 0.1$, and 36% with $\lambda_B = 10$. In HN, the gain of MD-CoMP over No-CoMP is even higher for the 5th percentile normalized goodput, which is improved by 425%, while for the average normalized goodput, the improvement is 14%, less than that achieved in RN. This is because in the HN, the MSs with the worst No-CoMP efficiency are those at the intersection of 3 cells, and the ICI is largely dominated by the 2 adjacent cells. Thus, MD-CoMP can mitigate these 2 major interferences and strongly reduce the ICI. However, as seen in previous figures, MD-CoMP in HN is very efficient for a smaller number of MSs than in RN.

Note that in the interference limited case, globally modifying the transmit power by a common factor has no impact on the performances neither, since the SIR would also remain constant. To go over the interference-limited bounds, one has to tune the transmit power of the BS, for example using HetNets, where different tiers of BSs have different transmit power levels and different densities. This is currently under investigation and will be the focus of future publications. It should also be noted that the results in Fig. 6 are obtained with the assumption that there is sufficient frequency resource and no allocation is carried out. If the bandwidth is fixed, practical allocation is employed, and the total system throughput is concerned, conclusions might be different.

5) Impact of Limited Clustering: Next, a performance comparison is carried out between a predefined clustering and the user-centric adaptive clustering. The planning of the predefined clustering is performed using an overlaying Voronoi tessellation, generated by the random placement of cluster centers [1] using a PPP of density λ_C ("PPP clustering"), which is based on BSs' locations only, not user-centric and non-overlapping. All BSs located in a cluster cell defined by this tessellation belong to the same cluster C. To provide fair comparison, it is assumed that if the primary station b_i of MS i, b_i belongs to C, then the MS can choose any subset of C, the complementary subset acting as interference.

Fig. 7 shows the clustering topology with user-centric adaptive clustering and the PPP clustering, where blue region stands for the locations where MSs choose a cluster size of $|B| = 1$, cyan for $|B| = 2$, orange for $|B| = 3$ and red for $|B| \geq 4$. The cluster boundaries of the predefined, non-overlapping PPP are shown and follow the green tessellation. The cluster boundary areas are therefore not improved compared to the non-cooperating scenario, since the MSs cannot select the proper set of BSs to be served by. On the contrary, the user-centric adaptive clustering allows each MS to select the optimized set of BSs and there are no cluster boundaries. Thus the network can fully benefits from CoMP to improve cell-edges MSs.

To evaluate the loss of efficiency due to the limitation of clustering possibilities, Fig. 8 plots the CDF of MSs' normalized goodput in the RN, using the PPP clustering with various densities of cluster centers and the user-centric adaptive clustering. It

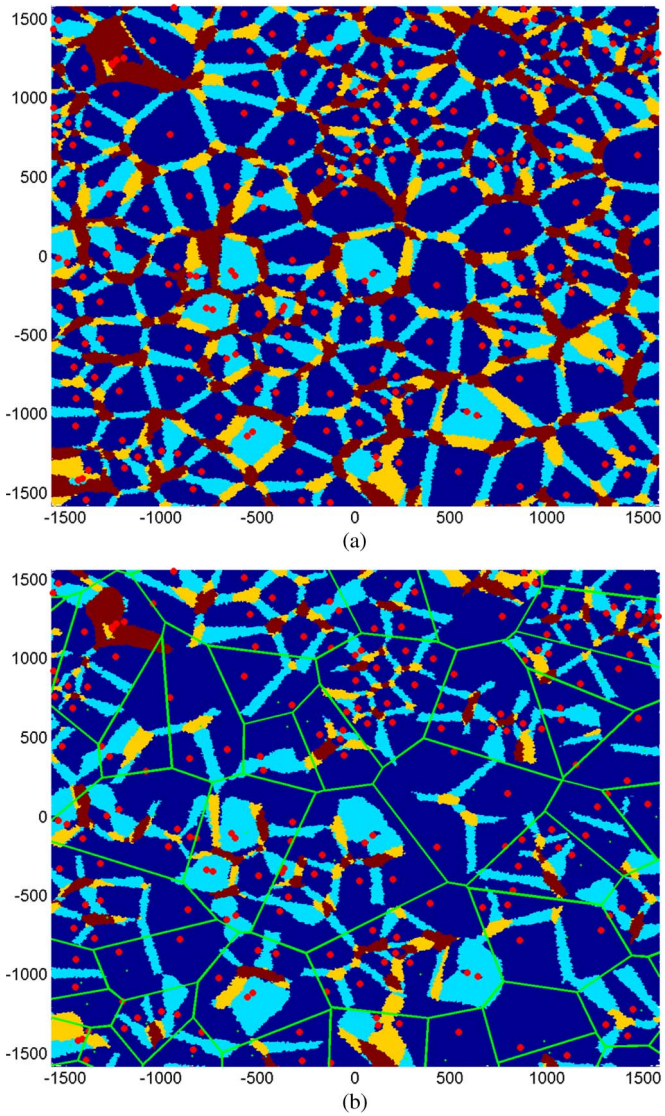

Fig. 7. Example of topology with CoMP. Red points are the BSs. Dark blue, cyan, yellow, and dark red areas are for MS locations that choose a cluster size of $|B| = 1$, $|B| = 2$, $|B| = 3$, $|B| \geq 4$, respectively. (a) User-centric adaptive clustering. (b) PPP clustering.

is shown that the performance of PPP clustering improves when the ratio λ_B/λ_C grows, since the clusters include more BSs. Thus, not only the MSs are able to select more BS in general but they also can select more suitable neighboring BSs. This reduces the cluster-edge area in the network. When λ_B/λ_C is increased to the maximum value, i.e., when all BSs in the network are in one cluster, the PPP clustering scheme should be identical to the adaptive one.

VI. Conclusion

This paper has investigated the performance of MD-CoMP in dense cellular networks. First, normalized goodput was defined as a proper metric to evaluate the performance of MD-CoMP. Next, the network SINR outage performance MD-CoMP was analyzed with fixed clustering. Then, the user-centric adaptive clustering was presented. By means of numerical calculation and simulations, the analytical network SINR outage

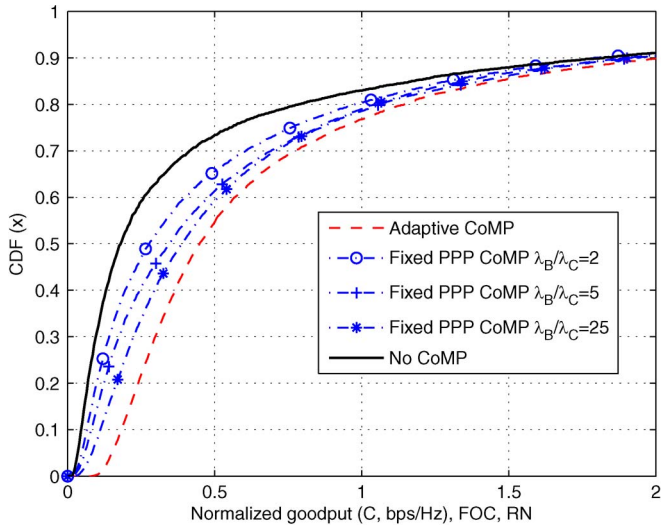

Fig. 8. CDF of the MSs' normalized goodput. The PPP clustering is shown for the ratio $\lambda_B/\lambda_C = 2, 5, 25$.

probability was verified. Moreover, considering normalized goodput, the performance of MD-CoMP with user-centric adaptive clustering was investigated in various scenarios. It can be concluded that

1) The network coverage is significantly improved by MD-CoMP, in both RN and HN topologies. It has been shown that the coordination of four BSs can improve the 10th percentile of SINR by 12 dB.
2) The distribution of optimal cluster sizes is quite different in RN and HN. Due to the irregular topology, RN can benefit more from MD-CoMP than HN. 78% MSs in RN would choose CoMP to optimize their normalized goodput while this number is 58% in HN. MSs in HN needing CoMP mostly choose a cluster size of two or three. In RN, the distribution is much less concentrated and about 40% MSs would employ a cluster size larger than three. This demonstrates the necessity to deploy user-centric adaptive clustering in RN.
3) Not only the MD-CoMP is chosen by more MSs in the RN than in the HN, but also its usage allows the MSs to experience higher capacity improvement. For instance, 58% MSs in RN could have their normalized goodput doubled by using MD-CoMP with the adaptive clustering over no-CoMP while this number is 36% in HN.
4) User-centric adaptive clustering outperforms any fixed or predefined clustering in both RN and HN. With the adaptive scheme, there is no cluster edge as with PPP clustering where the MSs' performance is poor due to the limited choices of clustering BSs.

Appendix
Proof of Theorem 1

Given a set of cooperation B_i, the $|B_i|$ closest BSs act as cooperating set, and thus the remaining BSs act as interferer. The interference $I_{r_{|B|}}$ then comes from the out-of-cluster BSs that are randomly located outside the circle of radius $r_{|B|}$ ($r_{|B|}$ is the distance to the farthest cooperating BS).For a given

value of the interference $I_{r_{|B|}}$ and assuming Rayleigh fading for the set of cooperation signals ($|f|^2$ follows a Chi-square distribution), the outage probability of the MD-CoMP SINR can be obtained using the distribution of the weighted sum of Chi-square random variables [22]

$$\mathbb{P}\left\{\gamma(B) > \gamma^* | I_{r_{|B|}}, r_b, \forall b = [1, |B|]\right\} = \sum_{b=[1,|B|]} \frac{e^{-\mu\gamma^*\left(\sigma_z^2 + I_{r_{|B|}}\right) r_b^\eta}}{\prod_{j=[1,|B|], j\neq b}\left(1 - \frac{r_j^{-\eta}}{r_b^{-\eta}}\right)}. \quad (11)$$

Then, by considering the total interference as a random variable, the SINR distribution is the average over all interference level and is expressed as

$$\begin{aligned}\mathbb{P}\left\{\gamma(B) > \gamma^* | r_b, \forall b = [1, |B|]\right\} &= \mathbb{E}_{I_{r_{|B|}}}\left(\sum_{b=[1,|B|]} \frac{e^{-\mu\gamma^*\left(\sigma_z^2 + I_{r_{|B|}}\right) r_b^\eta}}{\prod_{j=[1,|B|], j\neq b}\left(1 - \frac{r_j^{-\eta}}{r_b^{-\eta}}\right)}\right) \\ &= \sum_{b=[1,|B|]} \frac{L_{I_{r_{|B|}}}\left(\mu\gamma^* r_b^\eta\right) e^{-\mu\gamma^*\sigma_z^2 r_b^\eta}}{\prod_{j=[1,|B|], j\neq b}\left(1 - \frac{r_j^{-\eta}}{r_b^{-\eta}}\right)}, \end{aligned} \quad (12)$$

where $L_{I_{r_{|B|}}}(s) = E_{I_{r_{|B|}}}(\exp(-sI_{r_{|B|}}))$ is the Laplace transform of the interference received by the mobile from the stations located outside the disk centered at the mobile and of radius $r_{|B|}$. Focusing here on an exponentially distributed fading (e.g., the Rayleigh fading case), the expression of $L_{I_{r_{|B|}}}(s)$ has been derived in [2, Eq. (21)], exploiting the random properties of the PPP

$$L_{I_{r_{|B|}}}(s) = \exp\left(-2\pi\lambda_B \int_{r_{|B|}}^{\infty}\left(1 - \frac{\mu}{\mu + sv^{-\eta}}\right) v\mathrm{d}v\right). \quad (13)$$

In the non-cooperative communications, the only transmitting BS is located exactly at this distance of exclusion, which simplifies the derivation. In our case, the distance of exclusion for the interference is the distance $r_{|B|}$, while the transmitting stations are located at different distances ($r_b \leq r_{|B|}, \forall b \in B$). Following (12) and (13), we evaluate

$$\begin{aligned} L_{I_{r_{|B|}}}\left(\mu\gamma^* r_b^\eta\right) &= \exp\left(-2\pi\lambda_B \int_{r_{|B|}}^{\infty}\left(1 - \frac{\mu}{\mu + \mu\gamma^* r_b^\eta v^{-\eta}}\right) v\mathrm{d}v\right) \\ &= \exp\left(-2\pi\lambda_B \int_{r_{|B|}}^{\infty} \frac{\gamma^*}{r_b^{-\eta} v^\eta + \gamma^*} v\mathrm{d}v\right). \end{aligned} \quad (14)$$

Using the change of variable $u = \left(v/r_b(\gamma^*)^{1/\eta}\right)^2$, and note $\Gamma_\eta^* = (\gamma^*)^{2/\eta}$ for readability, we obtain

$$\begin{aligned} L_{I_{r_{|B|}}}\left(\mu\gamma^* r_b^\eta\right) &= \exp\left(-\pi r_b^2 \lambda_B \Gamma_\eta^* \int_{\frac{r_{|B|}^2}{r_b^2\Gamma_\eta^*}}^{\infty} \frac{\mathrm{d}u}{1 + u^{\eta/2}}\right) \\ &= \exp\left(-\pi r_b^2 \lambda_B \rho_\eta\left(\Gamma_\eta^*, \frac{r_{|B|}}{r_b}\right)\right), \end{aligned} \quad (15)$$

with $\rho_\eta(\Gamma_\eta^*, x) = \Gamma_\eta^* \int_{x^2/\Gamma_\eta^*}^{\infty} (1/(1 + u^{\eta/2}))\mathrm{d}u$.

Using again the RN properties, one can derive the probability of the distance between all neighboring stations and the user. In particular, the joint PDF of all B nearest BS distance is [23]

$$f(r_1, \ldots, r_{|B|}) = e^{-\lambda_B \pi r_{|B|}^2} (2\lambda_B\pi)^{|B|} \prod_{b=1}^{|B|} r_b, \quad (16)$$

where $r_1, \ldots, r_{|B|}$ are real positive values. The global SINR distribution is therefore given by

$$\mathbb{P}\left\{\gamma(B) > \gamma^*\right\} = \mathbb{E}_{r_1,\ldots,r_{|B|}}\left(\sum_{b=[1,|B|]} \frac{L_{I_{r_{|B|}}}\left(\mu\gamma^* r_b^\eta\right) e^{-\mu\gamma^*\sigma_z^2 r_b^\eta}}{\prod_{j=[1,|B|], j\neq b}\left(1 - \frac{r_j^{-\eta}}{r_b^{-\eta}}\right)}\right). \quad (17)$$

Replacing the expectation in (17) by the integration of each distance from 0 to the next station's distance and using (16) as the joint PDF distribution completes the proof.

Note that $\rho_\eta(\Gamma_\eta^*, x)$ can be simplified for the ease of numerical evaluation when considering $\eta = 4$, which gives: $\rho_4(\Gamma_4^*, x) = \Gamma_4^*((\pi/2) - \tan^{-1}(x^2/\Gamma_4^*))$, where $\tan^{-1}(.)$ is the inverse tangent function and $\Gamma_4^* = \sqrt{\gamma^*}$. Rearranging $\rho_4(\gamma^*, x)$ into (15) gives

$$L_{I_{r_{|B|}}}\left(\mu\gamma^* r_b^4\right) = \exp\left(-\pi r_b^2 \lambda_B \sqrt{\gamma^*}\left(\frac{\pi}{2} - \tan^{-1}\left(\frac{x^2}{\sqrt{\gamma^*}}\right)\right)\right). \quad (18)$$

REFERENCES

[1] S. Akoum and R. W. Heath, Jr., "Multi-cell coordination: A stochastic geometry approach," in *Proc. IEEE 13th Int. Workshop SPAWC*, 2012, pp. 16–20.

[2] J. G. Andrews, F. Baccelli, and R. K. Ganti, "A tractable approach to coverage and rate in cellular networks," *IEEE Trans. Commun.*, vol. 59, no. 11, pp. 3112–3134, Nov. 2011.

[3] H. S. Dhillon, R. K. Ganti, F. Baccelli, and J. G. Andrews, "Modeling and analysis of k-tier downlink heterogeneous cellular networks," *IEEE J. Sel. Areas Commun.*, vol. 30, pp. 550–560, Apr. 2012.

[4] K. Huang and J. G. Andrews, "A stochastic-geometry approach to coverage in cellular networks with multi-cell cooperation," in *Proc. IEEE GLOBECOM*, 2011, pp. 1–5.

[5] J. G. Andrews, "Seven ways that HetNets are a cellular paradigm shift," *IEEE Commun. Mag.*, vol. 51, no. 3, pp. 136–144, Mar. 2013.

[6] R. W. Heath, Jr., M. Kountouris, and T. Bai, "Modeling heterogeneous network interference using Poisson point processes," *IEEE Trans. Signal Process.*, vol. 61, no. 16, pp. 4114–4126, Aug. 2013.

[7] S. Jing, D. N. C. Tse, J. B. Soriaga, J. Hou, J. E. Smee, and R. Padovani, "Multicell downlink capacity with coordinated processing," *EURASIP J. Wireless Commun. Netw.*, vol. 2008, no. 5, pp. 586878-1–586878-19, Apr. 2008.

[8] P. Marsch and G. Fettweis, "Static clustering for COoperative Multi-Point (COMP) in mobile communications," in *Proc. IEEE ICC*, 2011, pp. 1–6.
[9] J. Park, E. Song, and W. Sung, "Capacity analysis for distributed antenna systems using cooperative transmission schemes in fading channels," *IEEE Trans. Wireless Commun.*, vol. 8, no. 2, pp. 586–592, Feb. 2009.
[10] M. Xu, D. Guo, and M. Honig, "Two-cell downlink noncoherent cooperation without transmitter phase alignment," in *Proc. IEEE GLOBECOM*, Dec. 2010, pp. 1–5.
[11] A. D. Wyner, "Shannon-theoretic approach to a Gaussian cellular multiple-access channel," *IEEE Trans. Inf. Theory*, vol. 40, no. 6, pp. 1713–1727, Nov. 1994.
[12] J. Zhang, R. Chen, J. Andrews, A. Ghosh, and R. Heath, "Networked MIMO with clustered linear precoding," *IEEE Trans. Wireless Commun.*, vol. 8, no. 4, pp. 1910–1921, Apr. 2009.
[13] D. Lopez-Perez, I. Guvenc, G. De La Roche, M. Kountouris, T. Quek, and J. Zhang, "Enhanced intercell interference coordination challenges in heterogeneous networks," *IEEE Wireless Commun.*, vol. 18, no. 3, pp. 22–30, Jun. 2011.
[14] A. Papadogiannis, D. Gesbert, and E. Hardouin, "A dynamic clustering approach in wireless networks with multi-cell cooperative processing," in *Proc. IEEE ICC*, Beijing, China, May 2008, pp. 4033–4037.
[15] A. E. Lozano, R. W. Heath Jr., and J. G. Andrews, "Fundamental limits of cooperation," CoRR, abs/1204.0011, 2012.
[16] A. Goldsmith, *Wireless Communications*. Cambridge, U.K.: Cambridge Univ. Press, 2005.
[17] V. Garcia, N. Lebedev, and J.-M. Gorce, "Capacity-fairness tradeoff using coordinated multi-cell processing," in *Proc. IEEE VTC Fall*, Sep. 2011, pp. 1–5.
[18] V. Garcia, N. Lebedev, and J.-M. Gorce, "Capacity outage probability for multi-cell processing under rayleigh fading," *IEEE Commun. Lett.*, vol. 15, no. 8, pp. 801–803, Aug. 2011.
[19] V. Garcia, Y. Zhou, and J. Shi, "Load aware CoMP clustering and intercell resource allocation in dense cellular networks," in preparation.
[20] *M.2135-1 Guidelines for evaluation of radio interface technologies for IMT-Advanced*, ITU-R, Geneva, Switzerland, Dec. 2009.
[21] "Coordinated multi-point operation for LTE physical layer aspects," Sophia-Antipolis, France, 3GPP TR 36.819 (V11.0.0)) 09, 2011.
[22] D. Hammarwall, M. Bengtsson, and B. Ottersten, "Acquiring partial CSI for spatially selective transmission by instantaneous channel norm feedback," *IEEE Trans. Signal Process.*, vol. 56, pp. 1188–1204, Mar. 2008.
[23] D. Moltchanov, "Distance distributions in random networks," *Ad Hoc Netw.*, vol. 10, no. 6, pp. 1146–1166, Aug. 2012.

Virgile Garcia (SM'09–M'12) received the M.Sc. degree in telecommunications engineering and the Ph.D. degree in electrical engineering from the University of Lyon INSA de Lyon, Lyon, France, in 2008 and 2012, respectively. From 2012 to 2013, he worked as a Postdoctoral Researcher with the Institute of Computing Technology, Chinese Academy of Sciences, Beijing, China, where his research interests focus on dense wireless networks, interference management, multiple-input multiple-output, and self-organizing networks.

Yiqing Zhou (S'03–M'05–SM'10) received the B.S. degree in communication and information engineering and the M.S. degree in signal and information processing from Southeast University, Nanjing, China, in 1997 and 2000, respectively, and the Ph.D. degree in electrical and electronic engineering from The University of Hong Kong, Pokfulam, Hong Kong, in 2004. She is currently a Professor with the Wireless Communication Research Center, Institute of Computing Technology, Chinese Academy of Sciences, Beijing, China. She is the author of over 70 papers and book chapters in the areas of wireless mobile communications. She is the Associate/Guest Editor for IEEE TRANSACTIONS ON VEHICULAR TECHNOLOGY, IEEE JOURNAL ON SELECTED AREAS IN COMMUNICATIONS (Special issue on "Broadband Wireless Communication for High Speed Vehicles" and "Virtual MIMO"), *Wiley's Wireless Communications and Mobile Computing*, *Wiley's Transactions on Emerging Telecommunications Technologies*, and *Springer Journal of Computer Science and Technology*. She is also the Symposium Cochair of the 2014 and 2015 IEEE International Conference on Communications, the Technical Program Committee Cochair of the 2012 International Conference on Communications and Networking in China, the Tutorial Cochair of the 2013 IEEE Wireless Communications and Networking Conference and the 2014 IEEE/CIC International Conference on Communications in China, and the Workshop Cochair of the 2012 IEEE International Conference on Smart Grid Communications and the 2011 IEEE Global Communications Conference. She has also served many international journals as a Peer Reviewer and conferences as a TPC member.

Jinglin Shi (M'10) is currently the Director of the Wireless Communication Technology Research Center, Institute of Computing Technology, Chinese Academy of Sciences, Beijing, China. He is also a Visiting Professor with Beijing University of Posts and Telecommunications, Beijing, China; the University of Sydney, Sydney, N.S.W., Australia; the University of Wollongong, Wollongong, N.S.W.; and Macquarie University, Sydney. His research interests include wireless communications system architecture and management, wireless signal processing theory, and wireless communication baseband processor design. As a team leader, he led the development of time-division synchronous code-division multiple access, Worldwide Interoperability for Microwave Access, and Long-Term Evolution (LTE) protocol stack systems successfully. He is currently responsible for several national projects in broadband wireless communications, including LTE time-division duplexing baseband chip design and research on radio resource management techniques toward International Mobile Telecommunications-Advanced. He has published two books and over 100 papers in telecommunications journals and conference proceedings and has more than 30 patents granted. He has also served in the organizing and technical committees of numerous national and international conferences. He was the General Cochair of the 2012 International Conference on Communications and Networking in China (ChinaCom), and a member of the Technical Program Committees of the IEEE Wireless Communications and Networking Conference, the IEEE International Conference on Communications, the 2006 IEEE International conference on Wireless Broadband and Ultra Wideband Communications, the 2007 Seventh International Symposium on Communications and Information Technologies, and ChinaCom 2007/2009.